

Scientific Contributions Oil & Gas, Vol. 48. No. 3, October: 91 - 112

SCIENTIFIC CONTRIBUTIONS OIL AND GAS

Testing Center for Oil and Gas LEMIGAS

Journal Homepage:http://www.journal.lemigas.esdm.go.id ISSN: 2089-3361, e-ISSN: 2541-0520



Transient Simulation to Analyze Wax Deposition and Flow Pattern Behavior Along Tubing Under ESP Installation and Gassy Well Condition

Brian Tony¹, Steven Chandra¹, Rafael J. S. Purba², Muhammad Fadhlan Solihan², and Ega Dimas Saputra¹

¹Petroleum Engineering Department, Universitas Pembangunan Nasional "Veteran" Yogyakarta Padjajaran Condongcatur Street, Sleman, Yogyakarta 55283, Indonesia.

²Faculty of Mining and Petroleum Engineering, Bandung Institute of Technology Ganesha Street No. 10 Bandung, Indonesia.

Corresponding author: brian.tony@upnyk.ac.id

Manuscript received: June 20th, 2025; Revised: July 22th, 2025 Approved: July 25th, 2025; Available online: October 13th, 2025; Published: October 13th, 2025.

ABSTRACT - Wax deposition is a common phenomenon that restricts flow in tubing, causing production decline. In the studied well, this decline is linked to wax thickness increasing from 0.0021 inches (Day 1) to 0.0114 inches (Day 7), occurring as fluid temperatures drop below 153.5°F. An Electrical Submersible Pump (ESP) is used to address this, but it impacts thermal conditions and flow behavior, especially in gassy wells. Therefore, a transient simulation is required to analyze wax deposition and flow behavior under ESP installation. This study performs a 7-day transient simulation using OLGA 2022.1.0 on the "X" well, a gassy well (700 scf/bbl GOR) with 38% wax content, utilizing a 70-stage DN610 ESP. Results show wax deposition begins on Day 1 (max 0.0021 inches) and thickens to 0.0114 inches by Day 7. Flow patterns vary along the tubing: stratified flow is dominant from the pump setting depth to KOP, while slug flow dominates from KOP to the tubing head. Annular flow was observed at the tubing head on several days. Sensitivity analysis revealed that more ESP stages result in more wax deposition. This is because the ESP increases the production rate; as more oil flows, more contained wax precipitates and deposits. The least wax was observed in the scenario with no ESP. This work demonstrates how ESP-induced liquid holdup and slug/ annular transitions accelerate wax deposition and emphasizes the importance of transient simulation in predicting production risks.

Keywords: ESP, wax deposition, flow pattern, gassy well, stage.

© SCOG - 2025

How to cite this article:

Brian Tony, Steven Chandra, Rafael J. S. Purba, Muhammad Fadhlan Solihan, and Ega Dimas Saputra, 2025, Transient Simulation to Analyze Wax Deposition and Flow Pattern Behavior Along Tubing Under ESP Installation and Gassy Well Condition, Scientific Contributions Oil and Gas, 48 (3) pp. 91-112. DOI org/10.29017/scog.v48i3.1731.

INTRODUCTION

The process of oil production from a reservoir has many challenges, especially when it comes to production in the wellbore. Flow restriction is one of the problems that often occurs during production in the wellbore for a variety of reasons. Beyond technical aspects, the sustainability of production with ESP is also linked to the contribution of the upstream oil and gas sector to the national economy. Input-output analysis shows an increase in the multiplier value from 6.18 to 7.89 for oil, and from 4.98 to 6.56 for gas, highlighting the vital role of this sector as an economic driver. (Rakhmanto et al., 2025). Field studies emphasize that free gas conditions in wells significantly affect ESP reliability; therefore, pump redesign based on Wiggins IPR analysis and frequency/PSD sensitivity is required to reduce the risk of upthrust to below 50% (Kurniawan 2024). Reservoir performance evaluation using production data involving ESP-equipped wells was also conducted by Usman (2014), who emphasized the integration of IPR analysis and historical data to support field optimization decisions. Wax deposition is a typical phenomenon that happens when the temperature is reduced in the wellbore, leading to the precipitation and deposition of crude oil components on the surface pipeline or the wall of the tubing. This deposit of wax can cause flow restriction in the tubing, resulting in a decrease of oil production (Sousa, et al., 2019). Field studies have reported production losses up to 20-30% within the first weeks of wax onset and pressure drops exceeding 200 psi along tubing sections when deposition is not mitigated (Basem E., et al., 2022). These quantitative impacts emphasize the urgency of analyzing wax deposition dynamics. With the problem of production declines, artificial lift is introduced as a method that can obtain a high production rate by reducing the bottomhole pressure, which can increase the production pressure drawdown. (Guo et al., 2017). As one of the artificial lift types, Electrical Submersible Pump (ESP) is widely utilized in the oil industry due to its advantages and high efficiency. The work principle of the multistage centrifugal pump and the electrical motor of ESP can increase the pressure of the fluids in a well, thereby pushing it to the surface (Takacs 2009). While the primary function of the ESP is to improve the production rates, the installation of ESP also significantly impacts the thermal conditions and flow patterns within the tubing, especially when the discharged fluid by the ESP pump is under gassy conditions. These factors influence the occurrence

of wax deposition. Previous studies mainly relied on steady-state assumptions and single-phase correlations (Nura et al., 2025), which often fail to capture transient multiphase flow effects and their coupling with thermal profiles. Recent works (Jiangbo W., et al., 2025) highlight the importance of dynamic modeling, but integration between ESP operation, wax deposition, and multiphase flow transitions remains limited in the literature.

In this case, an analysis of ESP installation will be conducted to determine its influence on wax deposition. The flow pattern in the tubing will also be analyzed since it has an impact on wax deposition according to several studies. For instance, research by Gong et al. (2011) explains the wax deposition thickness under various gas-liquid phase velocities in intermittent and stratified flow. The simulations will focus on tubing sections of a well with ESP installation to determine the flow pattern and how much wax is contained in the tubing. The novelty of this study lies in its explicit use of transient OLGA simulation to couple wax deposition growth, ESP stage sensitivity, and gassy well multiphase flow patterns. Unlike earlier works, this research provides a dynamic, integrated perspective that clarifies how ESP-induced changes in stratified, slug, and annular regimes accelerate wax accumulation and production decline.

The objectives to be achieved in this study are:
1). To identify the flow pattern and amount of wax deposition that occurs along the tubing of "X" well under the installation of ESP; 2). To analyze the influence of ESP installation on the wax deposition and the flow pattern behavior.

METHODOLOGY

Data collection

Literature study is conducted to collect information regarding wax deposition in tubing, flow model in tubing, software use, and design of ESP. This information is obtained by studying reference books and journals. Data was collected from well production history, schematic, PVT, and ESP catalog.

Reservoir deliverability and wellbore flow performance analysis

Reservoir deliverability is performed by constructing an Inflow Performance Relationship (IPR) to determine the achievable oil production rate from the reservoir at a given bottom-hole

pressure. Wellbore flow performance is evaluated by constructing Vertical Lift Performance (VLP) to determine the achievable oil production rate from the well. The analysis was conducted using Prosper 15.0 software.

ESP design

Pump evaluation calculations for ESP design are conducted using several inputs, such as pump data, reservoir and fluid data, IPR and VLP correlation data, and depend on the pump design rate that falls within the operating range. Using software to calculate the required stages, head, and power of the pump, the type of pump can be selected. ESP evaluation can then be carried out by seeing the pump performance curve as well as the IPR curve to be combined, resulting in nodal analysis to obtain the production data that will be matched from the well production history.

Transient simulation and sensitivity analysis

After ESP has been designed and matched by well test data, a transient simulation is performed to see the formation of wax on the tubing section as well as the change in flow pattern along the tubing. With fluid PVT and wax that have been modeled in Multiflash as the input, a transient simulation is conducted using OLGA 2022.1.0 software. Sensitivity analysis is carried out on the simulation by changing several parameters of ESP to see their effect on the wax deposition and flow pattern along the tubing. This simulation is performed for several days to see the increments or changes that occur regarding the simulated parameter outputs. The workflow can be seen in Figure 1.

The observation was conducted in the "Z" platform and "Y" field, which is in the Offshore Northwest Java Block. The reservoir plays in the "Y" field is categorized as a sandstone reservoir with heavy oil type. "Z" platform has a single-stringed well named "X" well that produces from December 2022 from the A and B zones and is completed with ESP as an artificial lift.

The observation focuses on "X" well, which is an oil well that has a production performance of 902 bfpd and 531 mcfd according to the well test report conducted on August 11th, 2023, and the latest well test shows the performance of "X" well to have 378 bfpd and 280 mcfd on November 25th, 2023. Figure 2 shows the fluid rate and wellhead pressure trend by test date from the first well test to the latest well test conducted, which indicates a higher drop in fluid production from the latest well test. Flow restriction is the main problem of this lower production, and it may be due to wax that has already been deposited on the "X" well tubing and higher-produced gas that can alter the flow pattern along the tubing.

The fluid composition from reservoir zones (A and B) is considered to be waxy crude with a wax content value of 38% and WAT of 140°F according to the latest PVT report. With the WHP and WHT of 145 psia and 85°F consecutively according to the latest well test report, the transient simulation needs to be performed due to the concern that fluid temperature in the tubing of "X" well is already lower than WAT, thus may cause wax deposition to occur.

The reservoir fluids have a high solution GOR, which is 700 scf/bbl with a bubble point pressure of 2915 psig. Since "X" well is also considered to be a gassy well according to the previous statement, the use of ESP during the start of production requires a gas separator to address the higher gas content. In addition, the observation will focus on designing ESP in "X" well first to obtain the proper result that matches the actual data (latest well test), which will be explained in the following section. To design the ESP of a well, the inflow and outflow performance must be determined first. Well inflow performance or reservoir deliverability is evaluated using IPR, which represents the relations between flowing bottom-hole pressure and liquid production rate. The fluid properties data that is used to determine IPR are shown in Table 1. Since the perforation zone of "X" well has two layers (A and B), the IPR model that was used to be construct it is the Multi-Layer Inflow model that is available from Prosper 15.0 software, which combines the calculations of IPR of each layer. The Multi-Layer Inflow model for each layer combines both the Darcy inflow equation and Vogel method, with the information on reservoir properties attached in Table 2.

Darcy's equation is used under the condition above the bubble point since the fluid flow is a single phase, with the assumption that the flow is radial around the well. The Vogel method is used under the condition below the bubble point, and it is based upon the rate when the FBHP is equal to the bubble point as calculated by the Darcy equation. Furthermore, the Vogel method is selected since it was found to give reliable results for almost any well with a BHP below the bubble point of the crude (Takacs, 2009), and it is still widely used in the industry (Guo et al., 2017).

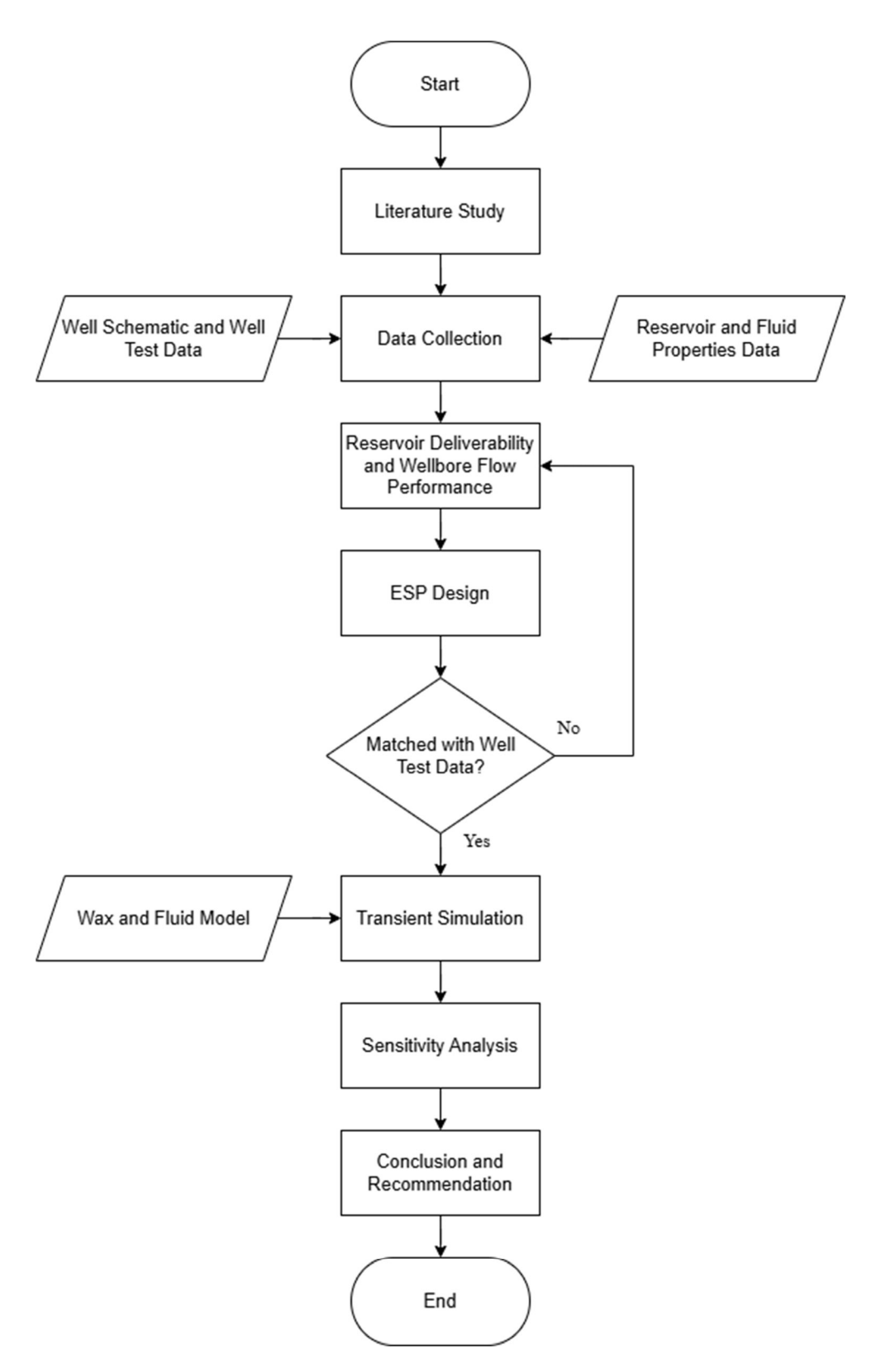


Figure 1. Workflow diagram

"X" well is a deviated well that has a trajectory data plotted in Figure 3, and the schematic data can be seen in Figure 4. The well also produces more gas since it has a high GOR, and the fluid will flow in the tubing after being discharged by the ESP pumps. The existence of gas in tubing will result in multiphase flow and the occurrence of flow patterns or flow regimes. Since the inclination angle of the "X" well and the fluid rate (gas and liquid) change along the depth of the tubing string, the flow pattern will also vary according to the conditions that cause it to occur. Therefore, multi-phase flow correlation is used instead of single-phase flow correlation.

Multi-phase flow correlation is used to predict liquid holdup and frictional pressure gradient, which will be the component of pressure losses occurring along the flow path that needs to be addressed by the discharge pressure of the ESP pump. Since the water cut is 1.3% according to the latest well test data, the oil and water are lumped together as one equivalent fluid for multi-phase flow correlation. Therefore, liquid-gas interaction is only to be considered, and the term is changed to two-phase flow correlation. The selected two-phase flow correlation is using Petroleum Experts 2 (PE-2), which is available from Prosper 15.0 software. This correlation combines the best features of existing flow correlations for the various flow patterns and can predict a low rate of wellbore flow performance (Prosper, 2018). PE-2 has also been tested to give better accuracy to construct wellbore flow performance compared to other models that are based on physical principles (Hasan et al., 2007). This correlation is used for wellbore flow performance calculations, as well as the latest well test data, which is shown in Table 3.

Simulation framework

To ensure that the transient simulation using OLGA 2022.1.0 and the ESP design evaluation remain consistent and representative of field conditions, several simplifying assumptions were adopted in this study:

Thermal boundary conditions: 1). steady-state radial heat transfer boundary condition was applied between the tubing and the surrounding formation; 2). Heat losses were assumed constant along tubing segments and do not account for seasonal variations.

Fluid and gas properties: 1). Gas solubility changes after ESP discharge were considered negligible, since the pressure drop across ESP stages is relatively small compared to reservoir pressure; 2). Reservoir fluid was modeled as a uniform composition based on the latest PVT data; compositional gradients along the wellbore were not included.

Wax properties: 1). Wax precipitation was modeled as having uniform composition and crystal growth kinetics along the tubing; 2). The Wax Appearance Temperature (WAT) was set at 153.5 °F based on laboratory PVT analysis and assumed constant during simulation.

Flow regime considerations: 1). Multiphase flow correlations (PE-2) were assumed to remain valid under both stratified and slug regimes; 2). Local flow instabilities below OLGA's resolution (e.g., micro-slugging) were not considered.

Operational Settings: 1). ESP motor heat generation was included as a constant value per stage, without accounting for frequency variation; 2). Gas separation efficiency was assumed at 60%, in line with catalog performance data. After ESP has been designed and matched with the well test data.

RESULT AND DISCUSSION

ESP design

The type of pump that is used for ESP installation is a REDA DN610 pump that has an operating rate ranging from 350 - 760 STB/day, since the targeted rate is 378 STB/day, and has a pump series of 400, meaning the OD for the pump is 4 inches, which is still below the ID casing. The calculated number of stages required for ESP is 70 stages, which can address the required head of 1660 ft. The gas separator is required since the "X" well is a gassy well type, and it is assumed this gas separator achieves a separation efficiency of 60% This assumption is justified because it falls within the typical offshore operating range of 40–70%. Sensitivity runs at 50% and 70% confirmed minimal effect (<0.0015 inches) on deposition thickness, so that it can handle the amount of gas entering the pump for a stable operation. Figure 5 shows the head performance curve of a 400 Series DN610 type pump with 70 stages for different pump operating frequencies. The selected operating frequency of 60 Hz gives the calculated pump operating point that is quite near the Best Efficiency Point (BEP). This operating point is selected to be higher than BEP rather than lower since it can give the operating rate

Fluid Rate vs Pressure Trend

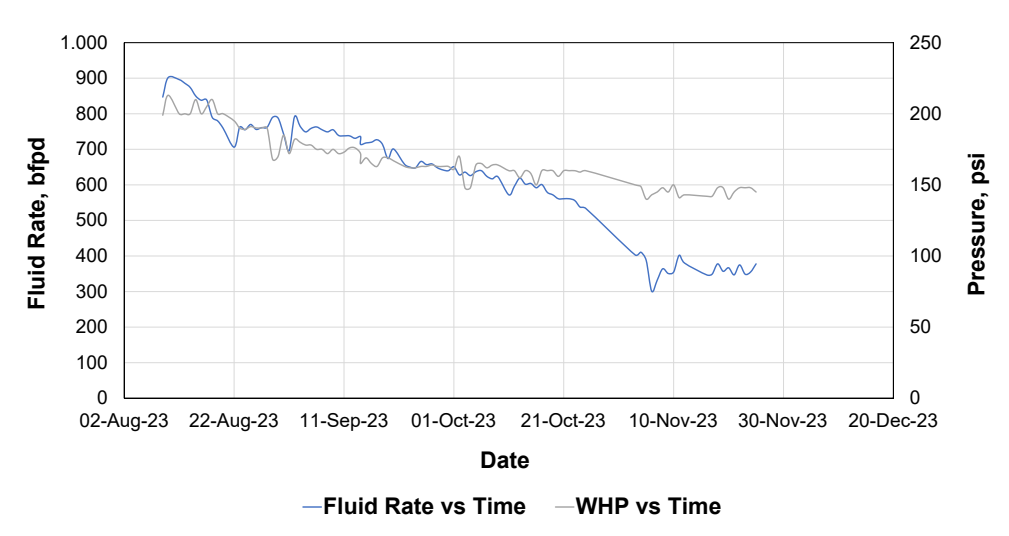


Figure 2. Fluid rate and WHP trend vs time of "X" well

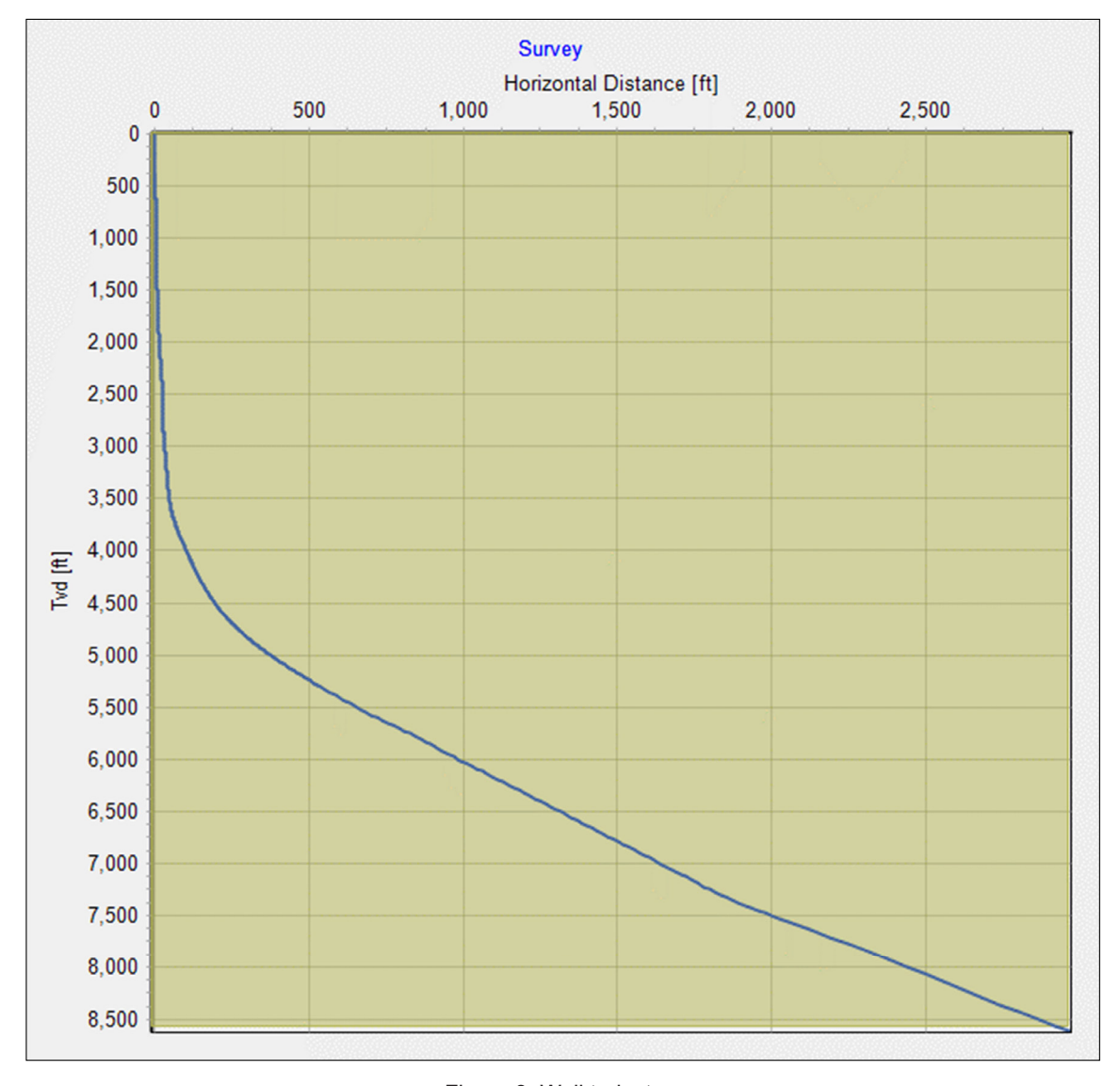


Figure 3. Well trajectory

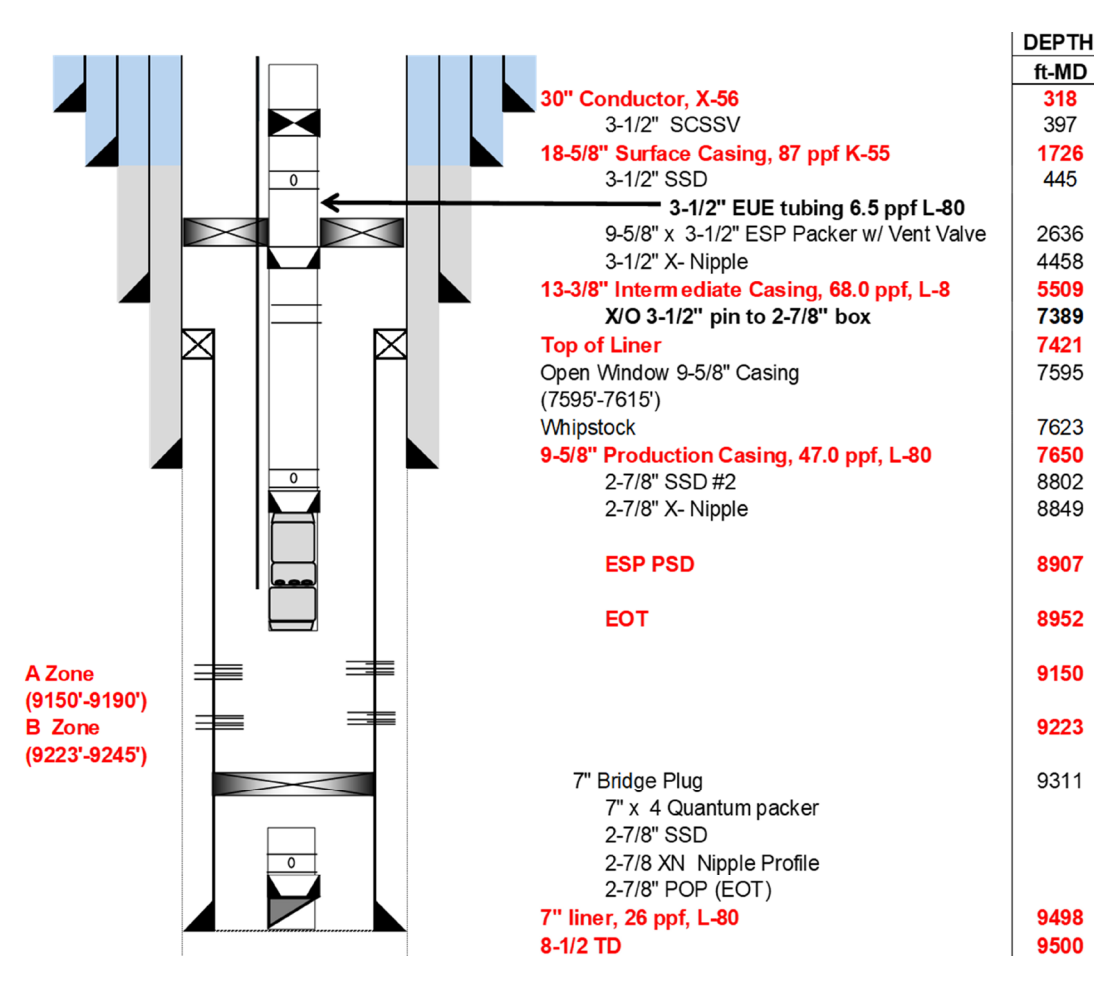


Figure 4. Well schematic

Table 1. Fluid properties of "X" well

Parameter	Value	Unit
Solution GOR	700	scf/STB
Oil Gravity	30	°API
Gas Gravity	1.1	
Water Salinity	15000	Ppm
Bubble Point Pressure	2915.02	Psig
Oil Viscosity @Pb, 284°F	0.44	cP
Mole Percent N ₂	0.04	cP
Mole Percent CO ₂	19.51	cP

Table 2. Reservoir properties of "X" well"

Parameter	Value	Unit
Reservoir Temperature	284	°F
Reservoir Pressure Layer A	3616	Psig
Reservoir Pressure Layer B	3639	Psig
Permeability Layer A	10.5	mD
Permeability Layer B	30.5	mD

Table 3. Latest well test data of "X well"

Parameter	Value	Unit
Test Date	November 25th, 2023	-
Liquid Rate	378	STB/day
Oil Rate	373	STB/day
Gas Rate	281	MMscfd
GOR	750.67	scf/STB
Water Cut	1.32	%
Wellhead Pressure	145	psia
Wellhead Temperature	85	°F

to be at BEP when it declines. The pump performance curve, shown in Figure 6, is the function of the pump rate that represents the head developed by the pump, the efficiency of the pump, and the horsepower required to drive the pump. The proposed design of ESP for the "X" well is a 400 Series DN610 type pump that has 70 stages, 57% pump efficiency, 60 Hz operating frequency, and 8 hp pump power required, which will be used for further transient simulation.

Nodal analysis

In order to check the suitability of the selected ESP design, nodal analysis is performed by taking into account the current actual installation, which is suited to the latest well test data. The reservoir properties will also be adjusted to match the performance with actual production data. Table 5 shows the adjusted reservoir properties in current conditions, with the IPR curve constructed with the input of current reservoir properties that are plotted

in Figure 7. "X" well is currently operating at a productivity index of 0.209 STB/d/psi as shown in Table 6 with an Absolute Open Flow (AOF) of 581.04 STB/d. To avoid redundancy, this AOF and operating range (174.3-406.8 STB/d) are consolidated in Table 6 and consistently referenced across all scenarios. The optimum rate range can be calculated with a rule of thumb of 30% - 70% of AOF. The result of the IPR/VLP curve is shown in Table 6 with an Absolute Open Flow (AOF) of 581.04 STB/d. The optimum rate range can be calculated with a rule of thumb of 30% - 70% of AOF, which is 174.3 - 406.8STB/day. The result of the IPR/VLP curve is shown in Figure 8, which gives the intersection of the two performance curves that define the operating point. Table 7 shows the result of system variables that have been calculated to be matched with the latest well test data, resulting in an appropriate value.

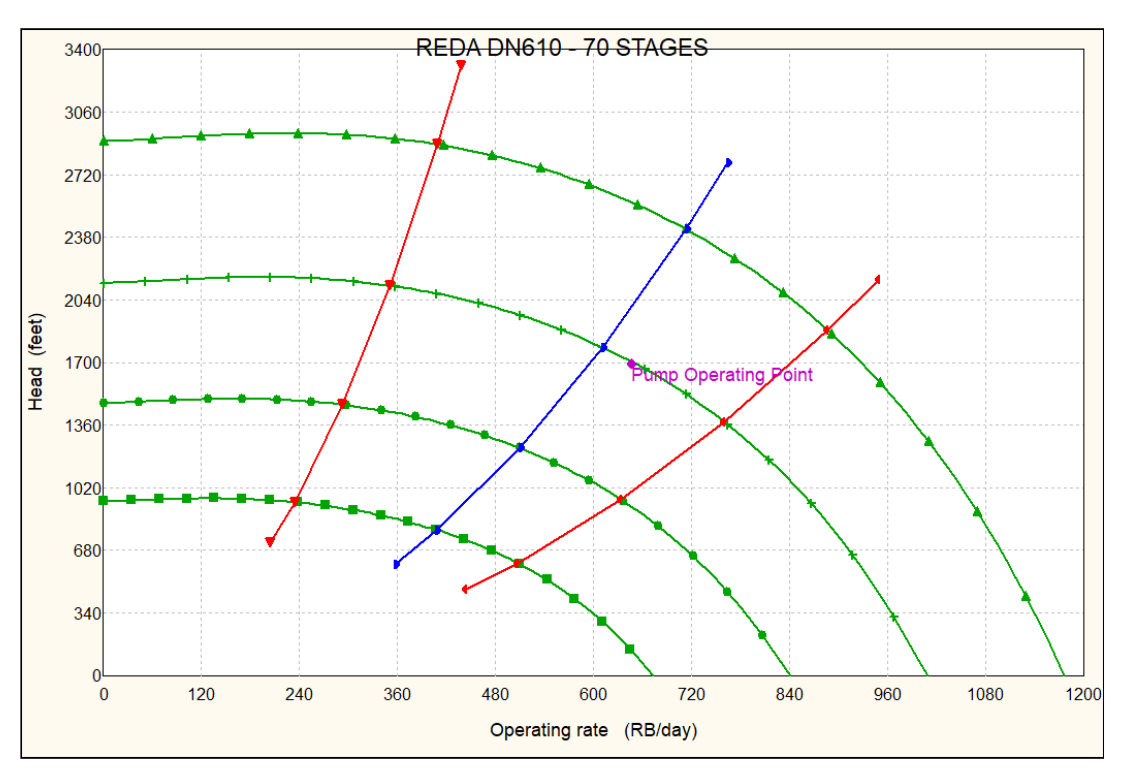


Figure 5. Head performance curve

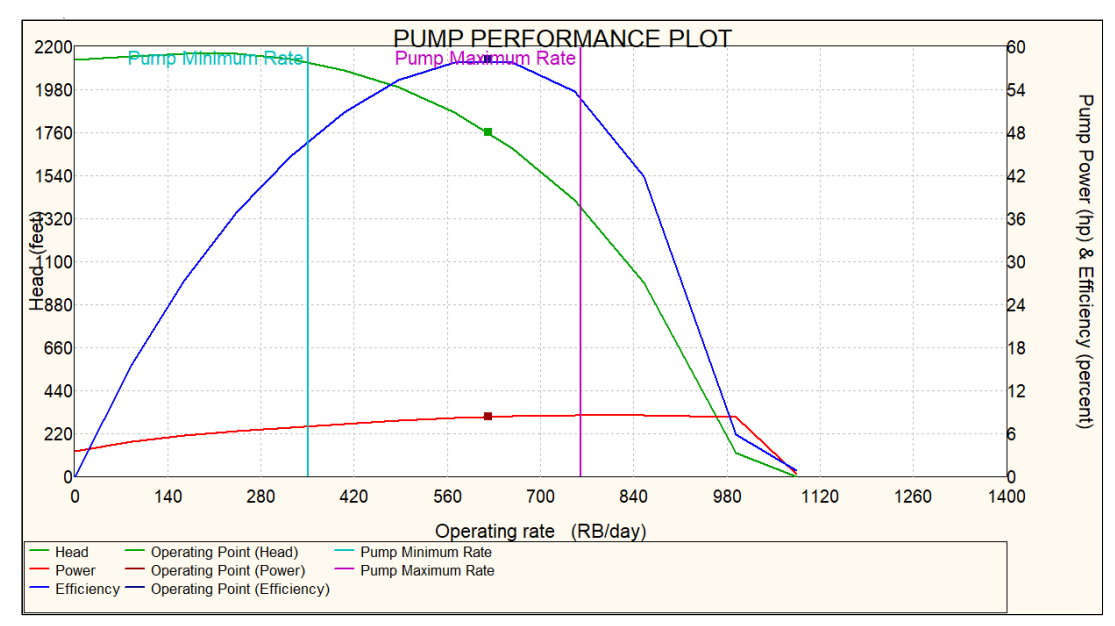


Figure 6. Pump performance curve

Performance simulation

The simulation is carried out with the base case scenario, that is, the initial simulation with all of the data that have been obtained and calculated in the previous discussion and without changing any parameters on them, for 7 days that have 5 outputs (day 1.4, day 2.8, day 4.2, day 5.6, and day 7). Care needs to be taken that OLGA outputs have different terms to read well depths. Table 8 below is used to

show the comparison between the actual depths and the OLGA depths in several parameters. Analysis of wax deposition, as well as flow pattern behavior for each day, is explained as follows:

Day 1.4

There is already a wax deposition on the first day of simulation, according to Figure 9, with it initially deposited at about 1677 ft-MD (about surface casing shoe area). It continues to deposit until it reaches the tubing head. The average and the maximum wax thickness deposited in the wall of tubing are consecutively 0.0012 inches and 0.0021 inches. The wax deposition that occurs on the first day of simulation is very low, considering the maximum

wax thickness deposited only covers 0.07% of ID tubing. From Figure 9, the temperature at which wax is first deposited is 153.1°F and continues to drop until the tubing head position, while the WAT at which wax is first deposited is 153.5°F and remains almost constant. This is the reason why

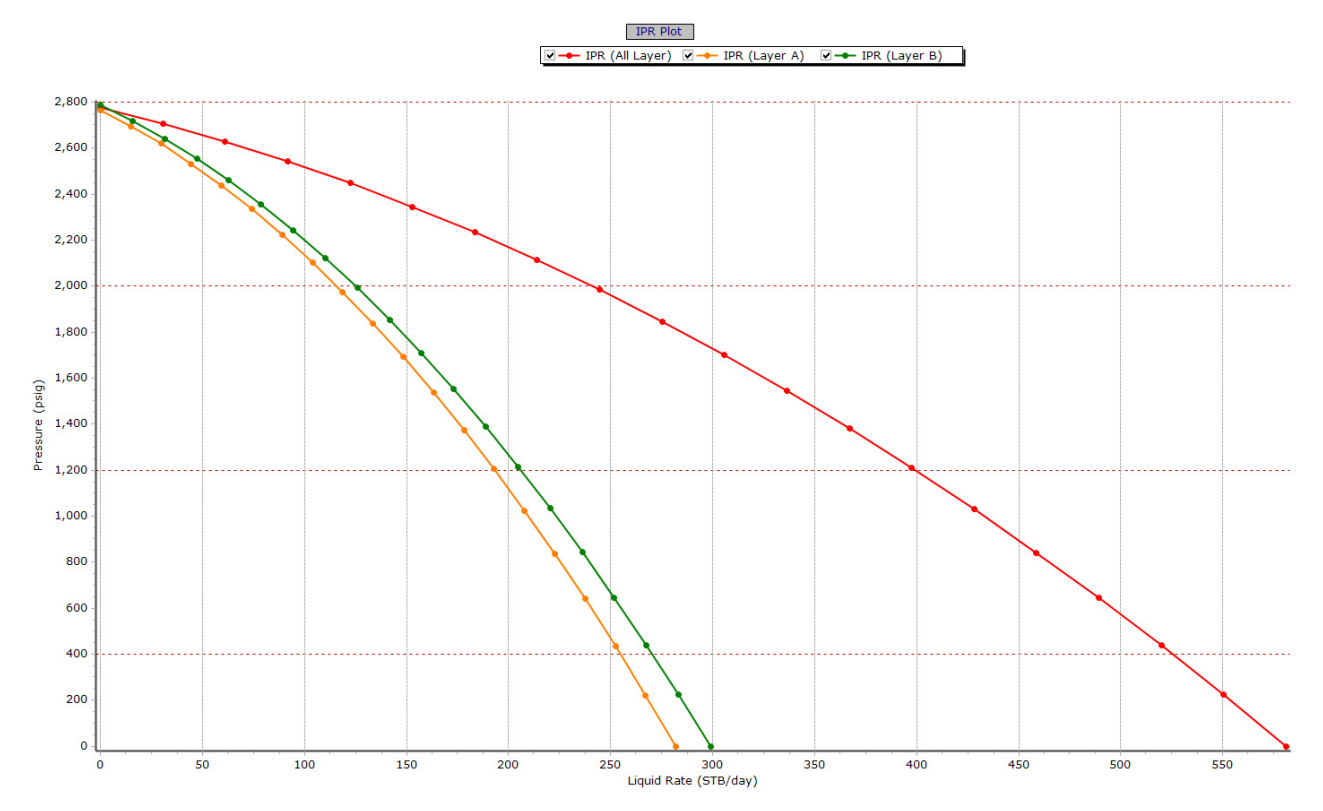


Figure 7. IPR curve of "X" well

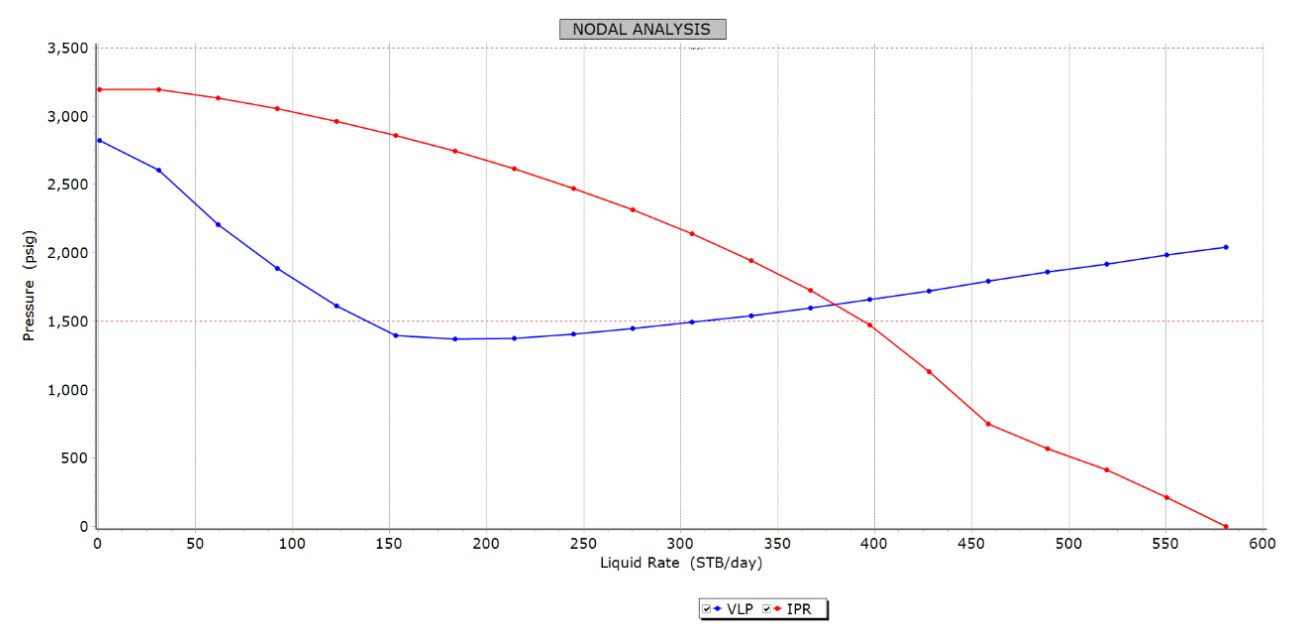


Figure 8. IPR/VLP curve of "X" well

Table 5. Reservoir properties at initial and matched condition of "X" well

Parameter	Initial Condition	Matched Condition
Reservoir Temperature (°F)	284	259
Reservoir Pressure Layer A (psig)	3616	2766
Reservoir Pressure Layer B (psig)	3639	2789
Permeability Layer A (mD)	10.5	5.5
Permeability Layer B (mD)	30.5	10.5
Skin Layer A	0	8
Skin Layer B	0	8

Table 6. Reservoir deliverability result of "X" well

Layer	PI (STB/d/psi)	AOF (STB/d)	Min. Rate (STB/d)	Max. Rate (STB/d)
Combined	0.209	581.04	174.31	406.73
A	0.102	282.03	84.61	197.42
В	0.107	299.01	89.70	209.31

Table 7. System variable result of "X" well

Parameter	Latest Well Test Data	Nodal Analysis Result
Liquid Rate (STB/day)	378	379.5
Oil Rate (STB/day)	373	374.5
Water Rate (STB/day)	5	5
Gas Rate (Mscfd)	280	281.1
WHP (psia)	145	145
WHT (°F)	85	94.6

Table 8. Depth Comparison between Actual Bottom MD of "X" Well to Pipeline Length on OLGA

Parameter	Actual Bottom MD (ft)	Pipeline Length on OLGA (ft)
Tubing Head Position	0	9498
Conductor Casing	318	9180
Surface Casing	1726	7772
Intermediate Casing	5509	3989
Production Casing	7650	1848
ESP PSD	8907	591
EOT	8952	546
A Layer	9190	308
B Layer	9245	253
TD	9498	0

wax deposition already occurs since the system temperature is already lower than WAT, which makes wax that is still in the produced crude oil begin to precipitate out and then continue to deposit in the wall of tubing. For the liquid and gas rates that can be seen in both Figure 9 and Figure 10, the liquid rate after discharge by the ESP pump continues to increase and then drop drastically, starting at the depth of 928 ft-MD (around surface casing area), and it has negative values (the liquid rate value that is measured

is below 0 STB/d). While the gas rate from the ESP pump setting depth to the tubing head position tends to increase. This can be explained by looking at the flow pattern that occurs along in the tubing.

At a pump setting depth to the depth of 5013 ft-MD (kick-off point), the flow pattern is stratified as can be seen from Figure 10, although the condition is not a horizontal state. But since the well at depths in that range is quite inclined and the liquid and gas have low flow rates, the separation of liquid and gas can still be happening with gravity, thus stratified flow is formed with the average liquid holdup of 0.7. Then, from the kick-off point (KOP) to a depth of 629 ft-MD (around surface casing area), slug flow is formed from significantly different densities at the higher liquid and gas rate, which characterizes the presence of liquid thin film, liquid slug, and Taylor bubble. As the pressure continues to drop, gas continues to be produced since it requires a lower pressure drawdown than liquid. This higher gas rate results in annular flow. The liquid is being pushed around the wall of the tubing by this fast-moving gas and forms a thin film that has slow movement. This gas moves upwards to the tubing head position while carrying the liquid in a thin film by shear force. However, the amount of liquid that moves downward is higher than that moves upward. This is possible because the pressure support required in lifting the liquid is lower than the gravity force that makes the liquid move downwards. So, the liquid in the surface casing area to the tubing head position has negative values.

Day 2.8

The result of the simulation on day 2.8 showed no significant differences beetween day 1.4 in wax deposition or flow pattern behavior. There is a thickening of wax deposition in the area at the same depth on day 1.4, according to Figure 11. With the initial deposition at the depth of 1677 ft-MD and continuing to deposit until at the tubing head, the average and the maximum wax thickness deposited in the wall of tubing are consecutively 0.0029 inches and 0.0053 inches, with it covering 0.18% of ID tubing. The temperature at which wax is first deposited, shown in Figure 11, is 153.8°F while the WAT is 153.6°F. The system temperature at initial wax deposition on this day is still above the WAT. This indicates that the initial wax deposition on day 2.8 is the wax deposition on the first day.

The liquid rate from Figure 11 and Figure 12 has the same behavior as day 1.4, but instead is more stable and then drops drastically at the depth of 823 ft-MD (around surface casing area) with it having negative values, while the gas rate tends to increase. Figure 12 shows the flow pattern behavior on simulation of day 2.8, which has a similar behavior to day 1.4. At the pump setting depth to the depth of 5013 ft-MD, the flow pattern is stratified flow with an average liquid holdup of 0.7. From KOP to the depth of 318 ft-MD (conductor casing shoe), slug flow is formed that has an average liquid holdup of 0.6 and an average liquid velocity of 0.46 ft/s. This indicates that the liquid slug remains small, and it moves quite slowly. Then, annular flow is formed from the depth of 257 ft-MD (around the conductor casing area) to the tubing head position, but, currently, both liquid and gas have negative values, which move downward

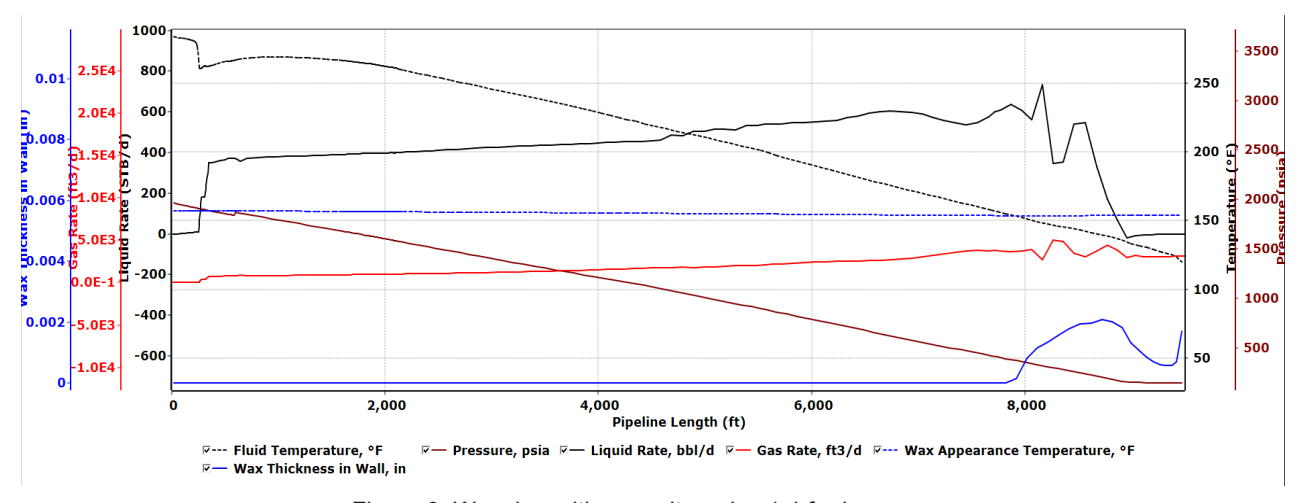


Figure 9. Wax deposition result on day 1.4 for base case

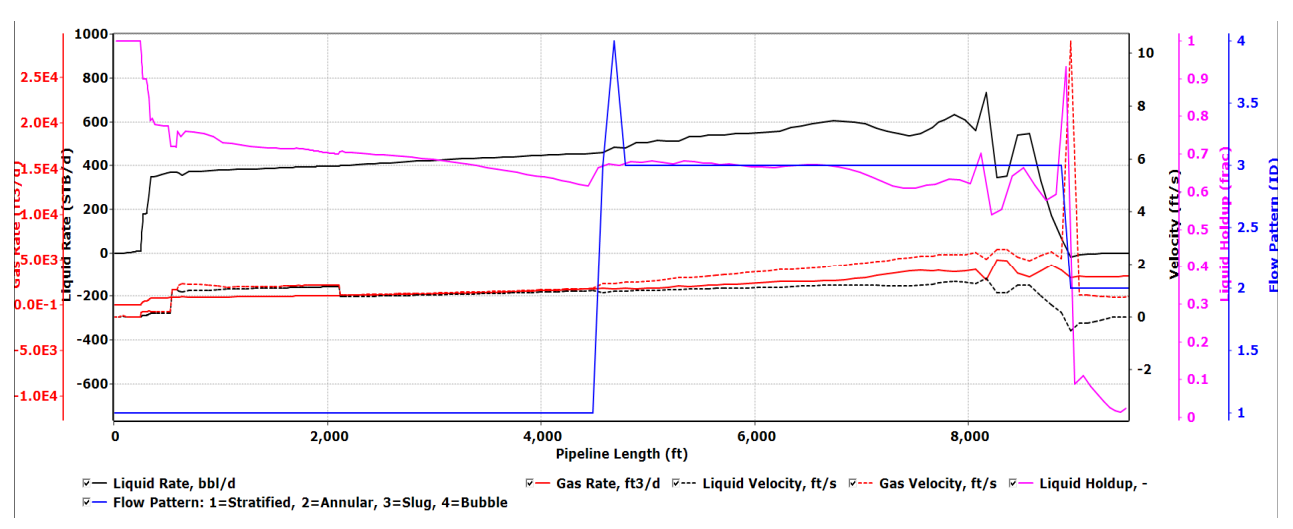


Figure 10. Flow pattern result on day 1.4 for base case

due to the gravity force. This annular flow happens because, in the previous simulation, the gas flows at a higher rate and moves with a higher velocity, which makes the annular flow to remain on day 2.8.

Day 4.2

On day 4.2, there is a thickening of wax deposition in the area at the same depth as the previous day, according to Figure 13. The initial wax deposition occurs at 1754 ft-MD (intermediate casing area) with a temperature of 152.7°F, which is lower than WAT and has a value of 153.4°F. The average wax thickness that is deposited on the wall of tubing is 0.0043 inches, and the maximum wax deposition thickness that occurs on this day is 0.0079 inches or about 0.26% of ID tubing. The flow pattern behavior on this day has a slight difference from the previous day, as can be seen in Figure 14. Starting at the pump setting depth to KOP, the flow pattern that occurs the most is stratified flow. But there is a brief slug

flow that occurs four times, at 8610 - 8697 ft-MD, 8349 – 8436 ft-MD, 5593 – 5680 ft-MD, and 5102 - 5186 ft-MD, which characterizes the presence of liquid slug body and the stratified region behind the slug (including gas pocket and liquid film). The flow remains slug after KOP until 1136 ft-MD (around surface casing area), which means the presence of a liquid slug body is increasing. There is also a long interlude of bubble flow that occurs at depths of 3470 – 3938 ft-MD (around the intermediate casing area). This indicates the gas pocket that formed in the previous slug flow breaks into small, discrete bubbles and then forms again into the new gas pocket at the next slug flow. Then, annular flow occurs until the tubing head position, which is characterized by fastmoving gas (high velocity) that flows at the center of the tubing while the liquid flows as a thin film around the wall of the tubing. The negative values of the liquid flow rate and velocity indicate a downward flow direction of liquid due to the gravitational force.

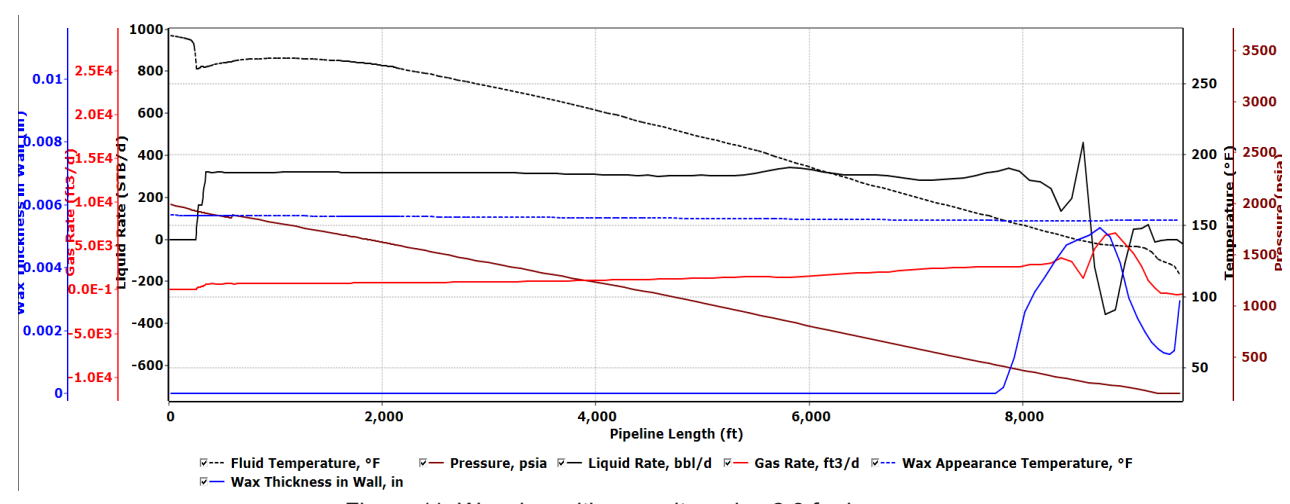


Figure 11. Wax deposition result on day 2.8 for base case

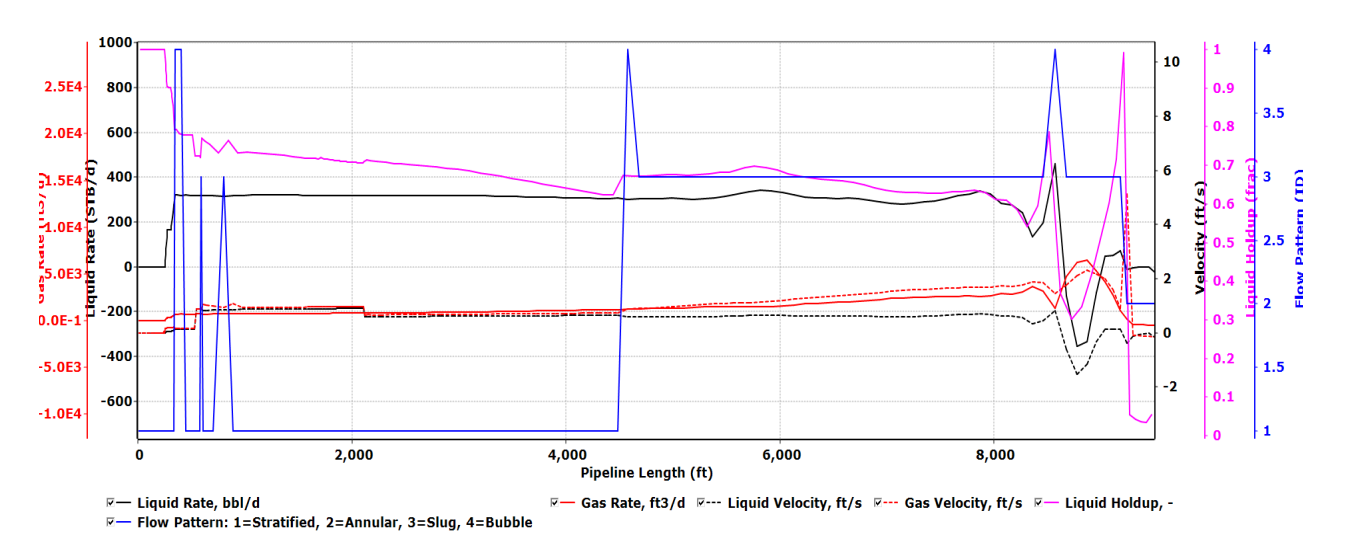


Figure 12. Flow pattern result on day 2.8 for base case

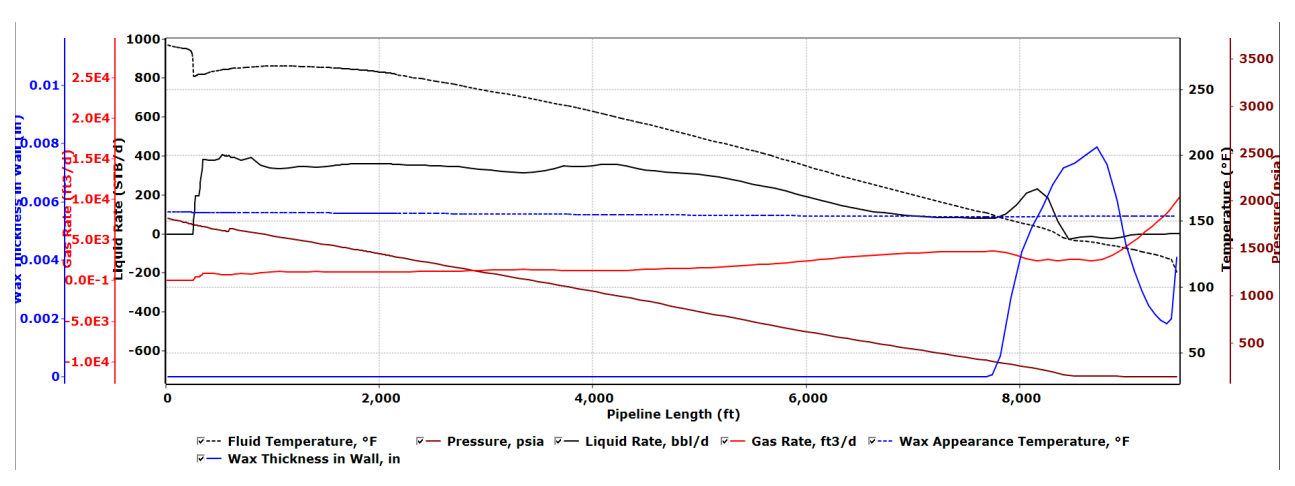


Figure 13. Wax deposition result on day 4.2 for base case

Day 5.6

The wax deposition result on day 5.6 can be seen in Figure 15, in which there is a thickening of wax deposition in the area at the same depth as on the previous day. The initial wax deposition occurs at 1754 ft-MD, same as day 4.2, with a temperature of 152.5°F, which is lower than WAT, which has a value of 153.6°F. The average wax thickness that is deposited on the wall of tubing is 0.0054 inches, and the maximum wax deposition thickness is 0.0097 inches or about 0.32% of ID tubing.

At this time, the liquid has a different behavior that can be seen in the flow pattern in Figure 16. Bubble flow is now formed at depths 6051 - 7302 ft-MD, while stratified flow still occurs from the pump setting depth to KOP. The gas phase in bubble flow is dispersed into smaller discrete bubbles as the velocity increases, resulting in the increased value

of liquid holdup as shown in Figure 16. The bubble flow occurs again after passing through KOP to a depth of 4816 ft-MD (around intermediate casing area) and from depths 2460 – 3366 ft-MD, where this flow occurs longer than day 4.2 with both liquid and gas having increased flow rates and velocities. Slug flow first occurred on this day at depths 3470 – 4816 ft-MD. It occurs again at a depth of 2359 ft-MD to the tubing head position. The slug flow that occurs on day 5.6 successfully carries liquid with a very high flow rate. This is because there are already more liquid slug bodies from the previous day, which then agglomerate and form a bigger liquid slug body. The obtained liquid rate at the tubing head is 926 STB/d.

Day 7

The wax deposition result on day 7 can be seen in Figure 17, with a thickening of wax in the area at the same depth on the previous day, as it continues

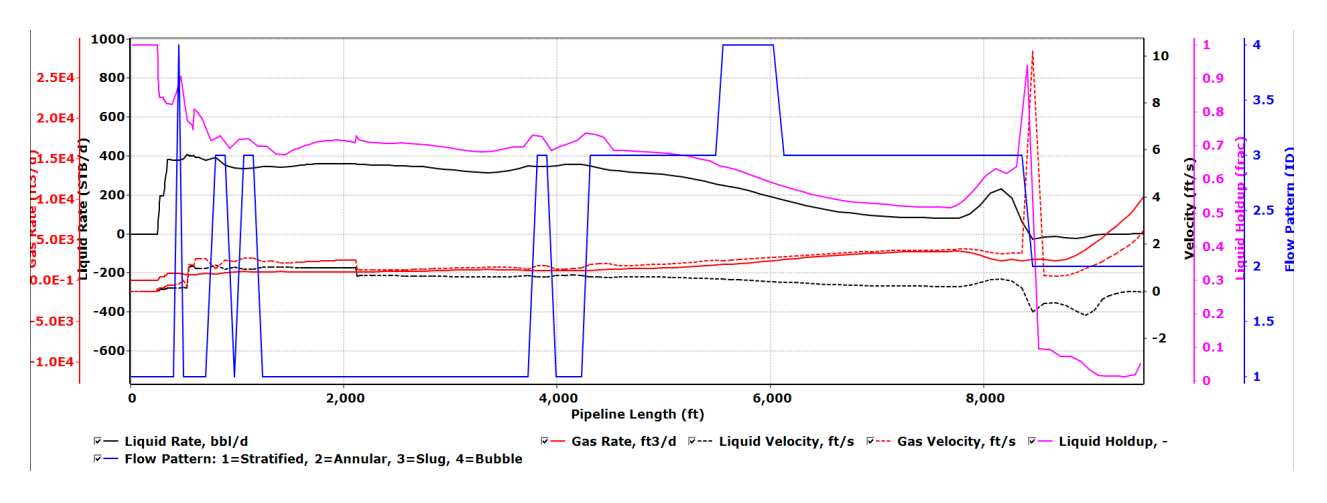


Figure 14. Flow pattern result on day 4.2 for base case

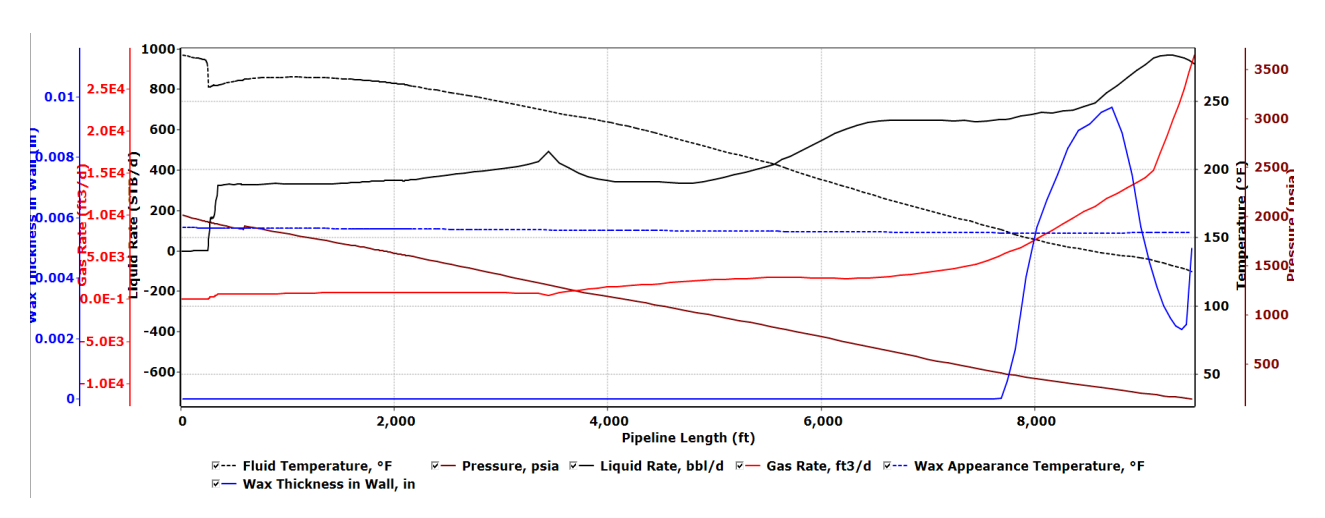


Figure 15. Wax deposition result on day 5.6 for base case

to deposit. The initial wax deposition occurs at 1809 ft-MD (around the intermediate casing area) with a temperature of 153.5°F, which is the same as WAT. The average wax thickness that is deposited on the wall of tubing is 0.0064 inches, and the maximum wax deposition thickness is 0.0114 inches or about 0.38% of ID tubing.

As for this day, the flow pattern shown in Figure 18 has a behavior that seems to return to the same pattern as the first day. Stratified flow occurs from the pump setting depth to KOP, while there is also slug flow that occurs between them (7665 – 8436 ft-MD). After KOP until at 928 ft-MD (around surface casing), slug flow occurs again with the intermittent bubble flow that forms at depths 3264 – 3366 ft-MD and 2961 – 3061 ft-MD. As the large liquid slug body has already lifted to the tubing head, the liquid in the slug flow starts over again to form a small slug body, and it is slower. Gas remains as usual; it continues to

increase until the flow is changed to annular, which is characterized by the high-moving gas that flows in the core of the tubing. The liquid is being pushed around again to the side of the tubing as a thin film. This liquid moves downward due to the gravitational force since the pressure support required to lift the liquid is not sufficient, resulting in negative values of flow rate and velocity. The phenomenon that happens on day 7 is similar to day 1.4, which indicates the cycle of slug body replenishment.

Sensitivity analysis

Sensitivity analysis is carried out within the transient simulation to see the effect of ESP installation on the wax deposition by changing several parameters that are divided into 3 cases.

Case A (Base case)

For the base case, the transient simulation for wax deposition has already been explained in the previous

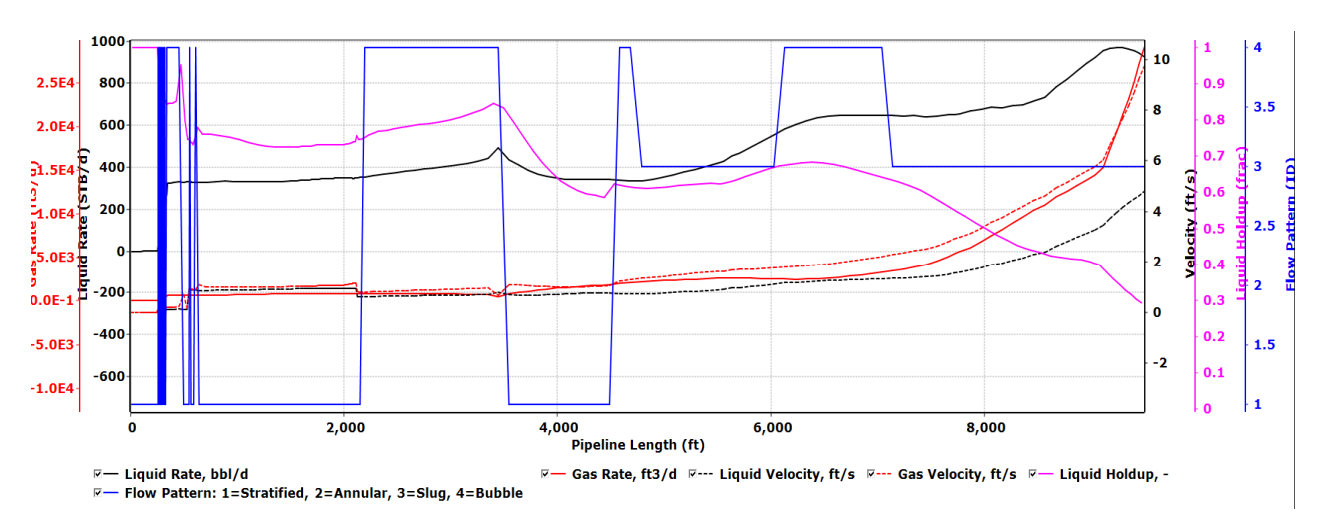


Figure 16. Flow pattern result on day 5.6 for base case

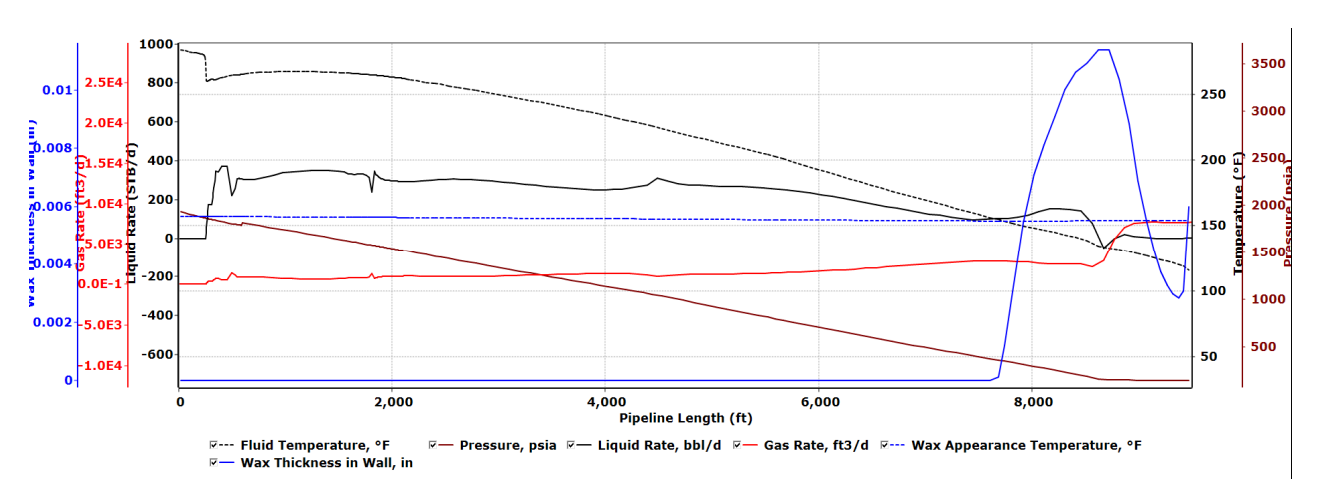


Figure 17. Wax deposition result on day 7 for base case

section. To summarize it from day 1.4 to day 7, Figure 19 shows the wax deposition that occurs from the first to the last day of simulation along the tubing for the base case. As the days passed, the amount of wax that was deposited increased, characterized by a thickening of the wax at the same depth. The maximum wax thickness that was deposited on the tubing from day 1.4 to day 7 is shown in Table 9. It is all located at 773 ft-MD (around surface casing area) with WAT that is quite stable. Day 2.8 has the highest increment of wax deposition at peak conditions. This can be seen from the fluid temperature which has the biggest drop compared to other days. This case will then be compared with another case based on changing parameters.

Case B (Change number of stages)

With ESP performance that is strongly influenced by the number of stages, Case B is conducted by changing the number of stages from the ESP pump base case (REDA DN610) with several stages. Transient simulation is then performed to see the wax deposition that occurs on the tubing. In this case, only the wax deposition from day 7 will be analyzed since it will be compared to the base case. The comparison between the wax deposition of Case A and Case B can be shown in Figure 20, while the data of wax deposition at peak condition, as well as the description of Case B, can be shown in Table 10. It is shown from the Figure that the more the number of stages increases, the more wax is deposited. But theoretically, adding more stages results in the addition of more heat from the ESP

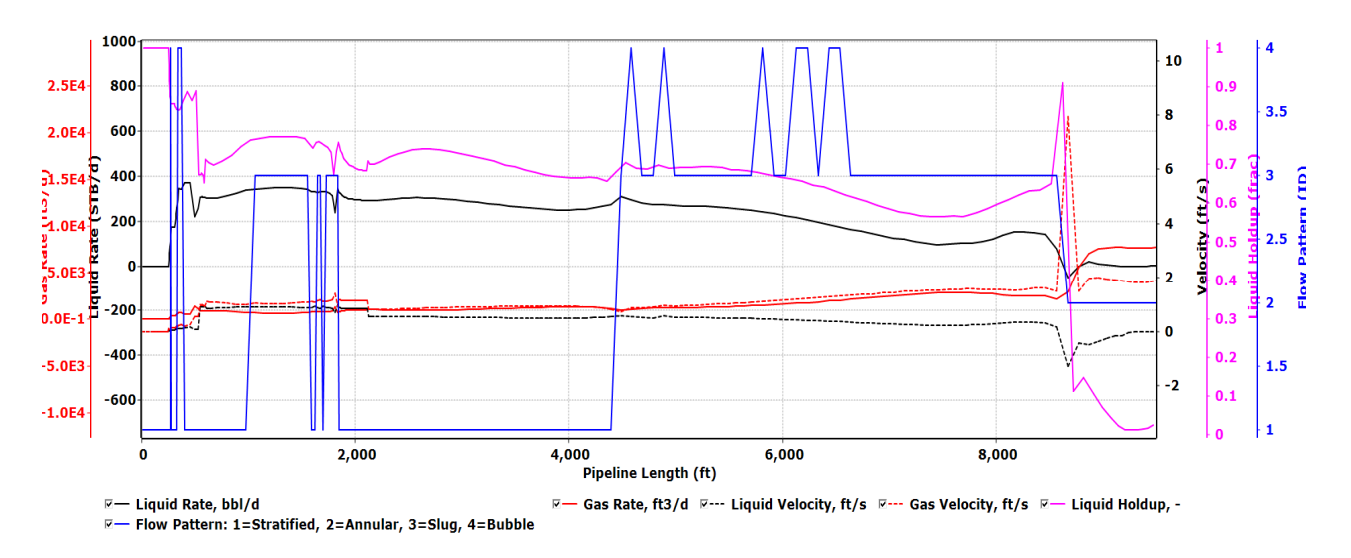


Figure 18. Flow pattern result on day 7 for base case

motor, which eventually makes the temperature of the tubing increase. As a result of this increasing temperature, the wax deposition on the tubing is reduced. However, the actual data from the transient simulation gives the opposite result. This phenomenon explains that adding more stages leads to more oil being produced. Increasing the amount of oil production can also increase the potential for wax to be deposited on the tubing, since the wax content from crude oil for all cases is the same and constant. The wax deposition itself depends on its deposition medium, which is tubing. The smaller the tubing ID, the more likely the wax will be deposited on the tubing because the tendency to fill the tubing surface is more easily. Since all of the cases have the same ID tubing (2.992 inches), by increasing the rate through adding more stages, the wax carried in the oil will also increase, and the possibility that wax will be deposited on the tubing will also increase.

Case C (Without ESP installation)

Case C is the case without ESP installation on it. Transient simulation is performed using the input parameters that are the same as the base case but without ESP. Wax deposition will be analyzed on day 7, same as Case B, to be compared with the base case. Case A (70 stages ESP) showed 0.0114 inches (0.38% ID), Case B (varied stages) ranged 0.0096–0.0123 inches (0.32–0.41% ID), while Case C (no ESP) was 0.0084 inches (0.28% ID). This highlights ESP's dual role: enhancing lift but accelerating deposition. The comparison between wax deposition that occurs in Case A and Case C can be shown in Figure 21,

while data on wax deposition at the peak condition of Case C can be shown in Table 10. In this case, the transient simulation gives a similar result to Case B, where using no ESP results in lower wax deposition compared to using ESP. Even though theoretically using ESP can generate more due to the ESP motor and mechanical friction in the pump stages, while this heat can raise the temperature of the fluid, which results in less potential of wax being deposited on the tubing, it has the same explanation as Case B. As the liquid, especially oil that is discharged by the ESP pump flows at a higher rate than without ESP, the wax, which is contained in that oil, that will be deposited on the tubing will also increase because the wax content on the oil is constant and with the more volume of oil is increase on the tubing, the more wax that will be able to precipitate and deposit. In Figure 21, the initial wax deposition in Case C occurs earlier than in Case A. The initial wax deposition on Case C occurs at a depth of 1890 ft-MD with the fluid temperature and WAT of 152.8°F and 153.4°F consecutively. The initial wax deposition on Case A occurs at a depth of 1809 ft-MD (around the intermediate casing area) with a fluid temperature of 153.5°F, which is the same as WAT. For that information, it is clearly stated that the wax deposition in Case C without ESP installation occurs early and with a temperature that is lower than Case A, so it can actually agree with the previous theory, even though Case A has more wax deposition on the tubing than Case C.

Suggestion of solution

The results of wax deposition and the flow pattern behavior from the transient simulation indicate several problems in the "X" well. First, the "X" well has already had wax deposition in the tubing since the first day of the simulation, although it is quite small. However, the deposition of wax will continue to occur as the fluid temperature is below WAT. Although ESP introduces motor heating, higher fluid velocity enhances convective cooling, and dynamic heat transfer modeling in OLGA confirmed that tubing wall temperature still falls below 153.5 °F. With that, it is only a matter of time until the wax deposition has a thickness that is close to the ID of the tubing, and eventually it can obstruct the flow of production. Second, from the flow pattern behavior, the liquid has a downward flow in the tubing (marked by a negative value of flow rate). If the liquid continues to fall back down to ESP, it can

damage ESP components. With all the problems that occur in the "X" well. The author proposes several solutions that can address the existing problems. Care needs to be taken that these are only suggestions and will not be discussed further in this study. For the first problem, the solution required is to conduct mitigation strategies for wax deposition. There are three methods according to Elarbe et al (2021): thermal, mechanical, and chemical methods. Since the wax that deposited on the tubing is in a vertical condition (after KOP), the scraper, as a mechanical method, can be used to remove the wax while it is economical and results in minimal formation damage (Allen, 1982). However, since the wax that formed is still low due to the simulation being only conducted until day 7, there are two ways of modeling wax deposition on the tubing. The first way is by conducting the transient simulation again, but this time it is extended to 1-2 months to see the wax thickness on the wall of the tubing. The problem with

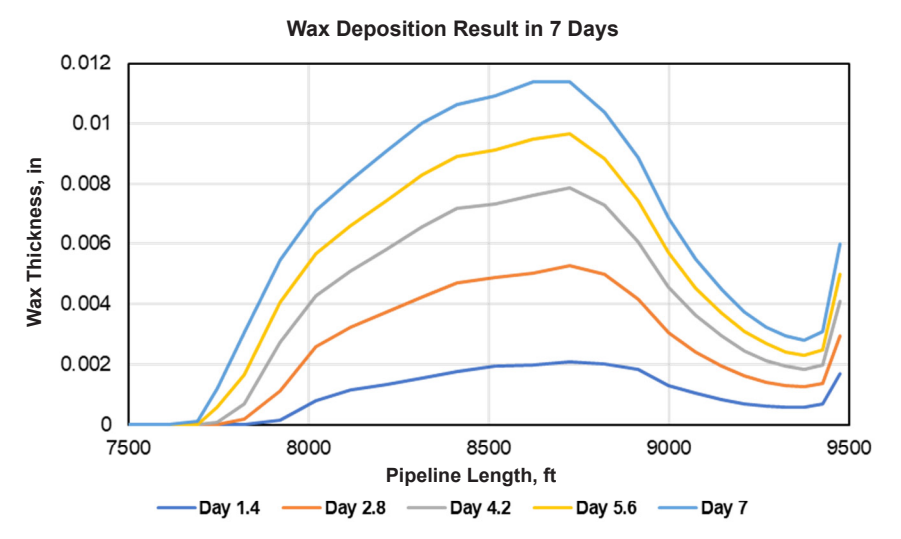


Figure 19. Wax deposition result in 7 days for base case

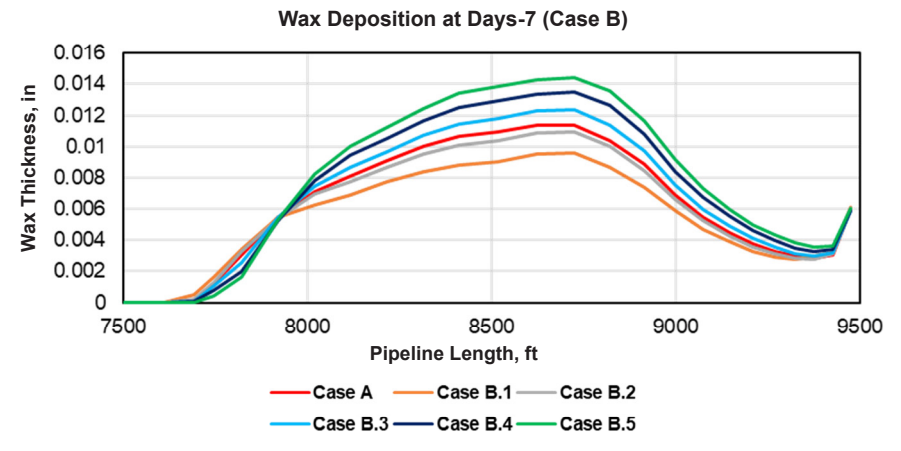


Figure 20. Wax deposition result on day 7 for case B

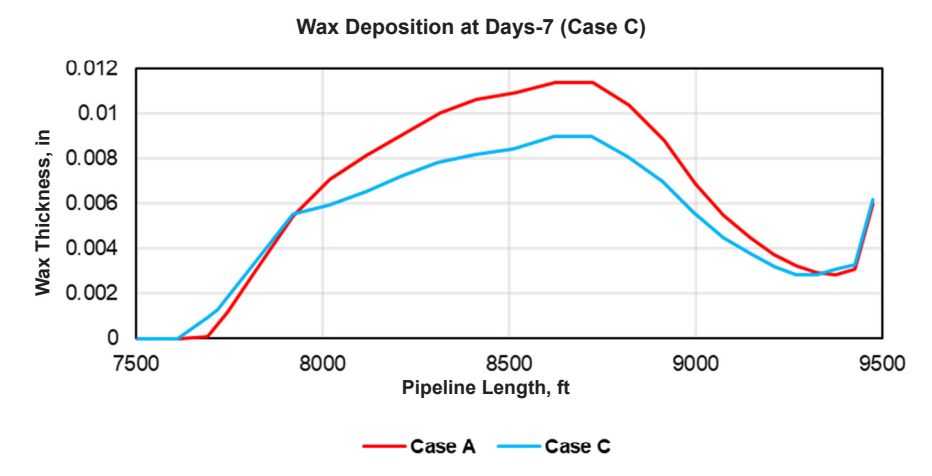


Figure 21. Wax deposition result on day 7 for case C

Table 9. Wax data at peak condition for base case

Timestamp	Maximum Wax Thickness (in)	Wax Increment (in)	Fluid Temperature (°F)	WAT (°F)	
Day 1.4	0.0021	-	139.4	153.7	
Day 2.8	0.0053	0.0032	136.4	153.6	
Day 4.2	0.0079	0.0026	133.5	153.9	
Day 5.6	0.0097	0.0018	132.8	153.6	
Day 7	0.0114	0.0017	132.8	153.9	

Table 10. Case description and wax data at peak condition for each case

Case	Description	Maximum Wax Thickness (in)	Fluid Temperature (°F)	WAT (°F)
Case A	Base Case	0.0114	132.8	153.9
Case B.1	Change Number of Stages (10 Stages)	0.0096	133.5	153.9
Case B.2	Change Number of Stages (50 Stages)	0.0109	139.7	153.7
Case B.3	Change Number of Stages (100 Stages)	0.0123	129.5	153.9
Case B.4	Change Number of Stages (150 Stages)	0.0135	138.2	153.5
Case B.5	Change Number of Stages (200 Stages)	0.0144	138.4	153.5
Case C	No ESP Installation	0.0084	138.2	153.7

the first way is that it takes a long time to model the wax deposition. The second way is by regression using the data of wax deposition from the first day to day 7, which gives a quicker result, but since it only uses 5 data points, the uncertainty using the regression method is quite high.

For the second problem, even though the liquid has a downward flow, there is one time when the liquid successfully flows to the tubing head position at a higher rate, and that is the time when the slug flow occurs with the liquid slug body in it. Since the process to get the slug flow is cyclic, the solution required is to change the continuous production to intermittent production. There are two solutions: the first one is to change the conventional ESP to intermittent ESP, and the second one is to change the artificial lift to intermittent gas lift. Intermittent ESP, according to Yudin et al (2022), can be modeled, and it is suitable for low-rate wells. The principle of intermittent ESP is by its cycle of turning on/off the pump equipment, while Variable Speed Drive (VSD) is used to allow the pump to be operated continuously or intermittently (Schlumberger, 2015; Yudin et al., 2022). However, there are no references that specifically discuss the implementation of intermittent ESP, so it has not yet been proven that intermittent ESP can be performed. The second solution is using the intermittent gas lift. Intermittent gas lift is the type of artificial lift where the gas is injected periodically into the tubing string whenever a sufficient length of liquid (liquid level) has accumulated at the bottom of the well. Then, a high volume of gas is injected below the liquid column, pushing the column to the surface as a slug. Gas injection is then stopped until a new liquid slug body of the proper column length builds up again. (Schlumberger, 2000). With many implementations and projects that have been carried out using the intermittent gas lift, this type of artificial lift is promising for "X" well. However, the availability of injection gas needs to be taken into consideration. Since the gas production of "X" according to the transient simulation that has been performed has only 29 Mscfd at its peak condition, the gas supply is required if "X" well uses intermittent gas lift as the artificial lift.

CONCLUSION

Based on the study that has been conducted, several conclusions have been obtained: 1). The flow pattern along the tubing of the "X" well under

ESP installation varied dynamically. From pump setting depth to KOP, stratified flow was dominant. From KOP to tubing head, slug flow was most frequent, while under higher gas fractions, the regime shifted to annular flow. These regime transitions directly influenced wax precipitation zonesl; 2). Wax deposition started at 1677 ft-MD and extended to 1809 ft-MD. The initial thickness was 0.0021 inches (0.07% ID) on Day 1.4, increasing to 0.0114 inches (0.38% ID) by Day 7. Maximum deposition occurred when fluid temperature fell below 153.5 °F, confirming Wax Appearance Temperature (WAT) as the key threshold; 3). ESP installation increased production rate but also accelerated wax deposition. Case A (70 stages ESP) reached a maximum wax thickness of 0.0114 inches, while Case B (50-100 stages) ranged from 0.0096 to 0.0123 inches. Case C (no ESP) showed a lower thickness of 0.0084 inches, despite reduced production. This confirms that higher ESP stages improve lifting efficiency but simultaneously intensify deposition risks; 4). A balance between production optimization and wax control is essential. While the ESP stage increase can sustain operation near Best Efficiency Point (BEP), it raises deposition risk along the tubing. Therefore, operational strategies such as stage optimization, intermittent ESP cycling, or complementary mitigation (e.g., chemical inhibition or thermal management) should be integrated to maintain both production continuity and well integrity.

ACKNOWLEDGEMENT

This work was supported by Universitas Pembangunan Nasional "Veteran" Yogyakarta and Institut Teknologi Bandung. The author acknowledges the support provided during the research, publication, and presentation of this paper. The writer receives input and recommendations.

GLOSSARY OF TERMS

Symbol	Definition	Unit
ESP	Electrical	_
	Submersible Pump	
WAT	Wax Appearance	°F
	Temperature	
OLGA	Dynamic Multiphase	_
	Flow Simulator	

IPR	Inflow Performance	_
	Relationship	
VLP	Vertical Lift	_
	Performance	
AOF	Absolute Open Flow	STB/day
PI	Productivity Index	STB/d/psi
BEP	Best Efficiency Point	_
GOR	Gas-Oil Ratio	scf/STB
WHP	Wellhead Pressure	psia
WHT	Wellhead	°F
	Temperature	
PVT	Pressure-Volume-	_
	Temperature data	
ID	Inner Diameter	in
OD	Outer Diameter	in
MD	Measured Depth	ft
KOP	Kick-Off Point	ft
PSD	Pump Setting Depth	ft
EOT	End of Tubing	ft
STB	Stock Tank Barrel	_
bfpd	Barrels of fluid per	bbl/day
	day	
mcfd	Thousand cubic feet	Mscf/day
	per day	
cp	Centipoise	cР
	(viscosity)	
mD	Millidarcy	mD
	(permeability)	
°API	API gravity of crude	_
	oil	

REFERENCES

- Ali, S. I., Lalji, S. M., Haneef, J., Khan, M. A., Yousufi, M., Yousaf, N., & Saboor, A. (2022). Phenomena, factors of wax deposition and its management strategies. Arabian Journal of Geosciences, 15(2), 133.
- Clegg, J. D., Bucaram, S. M., & Hein Jr, N. W. (1993). Recommendations and Comparisons for Selecting Artificial-Lift Methods (includes associated papers 28645 and 29092). Journal of Petroleum Technology, 45(12), 1128-1167.
- Kurniawan, D. H. (2024). Redesain Electric Submersible Pump (Esp) pada Sumur yang Mengandung Gas †œW-30†Lapangan †œAâ€. Lembaran publikasi minyak dan gas bumi, 58(1), 1-11. https://doi.org/10.29017/LPMGB.58.1.1610.
- Elarbe, B., Elganidi, I., Ridzuan, N., Abdullah, N.,

- & Yusoh, K. (2021). Paraffin wax deposition and its remediation methods on crude oil pipelines: A systematic review. Maejo International Journal of Energy and Environmental Communication, 3(3), 6-34.
- Gong, J., Zhang, Y., Liao, L., Duan, J., Wang, P., & Zhou, J. (2011). Wax deposition in the oil/gas two-phase flow for a horizontal pipe. Energy & Fuels, 25(4), 1624-1632.
- Guo, B., Liu, X., & Tan, X. (2017). Petroleum production engineering. Gulf Professional Publishing.
- Hao, L. Z., Al-Salim, H. S., & Ridzuan, N. (2019). A Review of the Mechanism and Role of Wax Inhibitors in the Wax Deposition and Precipitation. Pertanika Journal of Science & Technology, 27(1).
- Hasan, A. R., Kabir, C. S., & Sayarpour, M. (2007). A basic approach to wellbore two-phase flow modeling. In SPE Annual Technical Conference and Exhibition (pp. SPE-109868). Society of Petroleum Engineers.
- Jiangbo W., Yongrui L., Yuzhang J., Haijun L., Chuanlin Y., Zhenwei H., Chuyu W., and Yuxin L. (2025). Progress on Wax Deposition Characteristics and Prediction Methods for Crude Oil Pipelines. Processes.
- Kelland, M. A. (2016). Production chemicals for the oil and gas industry. CRC press.
- Nguyen, T., & Nguyen, T. (2020). Electrical Submersible Pump. Artificial Lift Methods: Design, Practices, and Applications, 107-179.
- Nura M., Donglin Z., Bingxing W., Mukhtar A., Muhammad U. G., 2025, New insights into wax deposition challenges: Experimental investigation across varied pipeline curvatures. Experimental Thermal and Fluid Science.
- Olga Dynamic Multiphase Flow Simulator. SLB. 2024, Retrieved from https://www.slb.com/products-and-services/delivering-digital-at-scale/software/olga/olga-dynamic-multiphase-flow-simulator/.
- Rakhmanto, P. A., Notonegoro, K., Setiati, R.,
 & Mardiana, D. A. (2025). Analysis on The Linkages and Multiplier Effects of The Upstream Oil and Gas Sector on Indonesia's Economy

- Using The Input-Output Method. https://doi. org/10.29017/scog.v48i1.1700.
- Prosper (2018). User Manual. Petroleum Experts Ltd.
- Schlumberger. 2000, Gas Lift Design and Technology. Chevron Main Pass 313 Optimization Project.
- Schlumberger (2015). Oilfield Review, 25(1).
- Shoham, O. (2006). Mechanistic modeling of gas-liquid two-phase flow in pipes. Society of Petroleum Engineers.
- Sousa, A. L., Matos, H. A., & Guerreiro, L. P. (2019). Preventing and removing wax deposition inside vertical wells: a review. Journal of petroleum exploration and production technology, 9, 2091-2107.
- Takacs, G. (2017). Electrical submersible pumps manual: design, operations, and maintenance. Gulf professional publishing.
- Theyab, M. A., & Yahya, S. Y. 2018, Introduction to wax deposition. Int J Petrochem Res, 2(1), 126-131.
- Pasarai, U. (2014). PRACTICAL METHOD FOR ASSESSING RESERVOIR PERFORMANCE TO REVIVE CLOSED OIL WELLS. Scientific Contributions Oil and Gas, 37(3), 161-174. https:// doi.org/10.29017/SCOG.37.3.637.
- Yudin, E., Piotrovskiy, G., Smirnov, N., Bayrachnyi, D., Petrushin, M., Isaeva, S., & Yudin, P. (2022). Modeling and Optimization of ESP Wells Operating in Intermittent Mode. In SPE Annual Caspian Technical Conference (p. D021S012R001). Society of Petroleum Engineers.